J Therm Anal Calorim (2018) 131:2213–2223
https://doi.org/10.1007/s10973-017-6783-5

Isothermal and nonisothermal cold crystallization kinetics of poly(L-lactide)/functionalized eggshell powder composites

Yi Li[1] · Changyu Han[2] · Yancun Yu[2] · Liguang Xiao[1] · Yan Shao[1]

Received: 17 July 2017 / Accepted: 24 October 2017 / Published online: 1 November 2017

Abstract Functionalized eggshell powder (NES) with nucleating surface of calcium phenylphosphonic acid (PPCa) for poly(L-lactide) (PLLA) was compounded with PLLA via melt blending to improve the cold crystallization process of PLLA. The cold crystallization behavior of the PLLA/NES composites was studied by differential scanning calorimetry. The isothermal cold crystallization rates have been enhanced obviously in the PLLA/NES composites than in the neat PLLA, indicative of the excellent nucleating effects of NES on PLLA. For the nonisothermal cold crystallization, the overall crystallization rate of PLLA increased with both increasing NES loadings and heating rate. It was found that the Avrami equation and the combined Ozawa–Avrami model could describe the experiment data successfully.

Keywords Poly(L-lactide) · Composite · Crystallization kinetics

Introduction

Poly(L-lactide) (PLLA) has been focused more and more because of its biodegradability, biocompatibility, renewability, and harmless to the human body. It has found wide applications in many fields including medical, food packaging, and agricultural [1, 2]. However, its shortcoming of slow crystallization rate and low mechanical properties greatly limits its wide applications [3, 4]. To overcome these problems, reinforced composite has been introduced [5, 6]. Compounding with fillers, such as layer silicate [7–9], carbon nanotubes (CNTs) [10–14], polyhedral oligomeric silsesquioxanes (POSS) [15–18], and eggshell powder [19], is an effective method to prepare PLLA composites with high performance.

It is well know that the physical and mechanical properties of polymer are largely affected by its level of crystallinity and solid-state morphology [20–22]. PLLA is mostly amorphous when subjected to injection molding or extrusion processing as a result of its slow crystallization rate [23, 24]. Therefore, in the development of the physical and mechanical properties of high-performance PLLA materials, it is recognized that cold crystallization process [annealing process higher than the glass transition temperature (T_g)] is very necessary to improve the degree of crystallinity. An understanding of the cold crystallization kinetic is of practical importance, because it is a key to cognize the relationship between properties and processing and control of the crystallizing factors allowing for the material design with good properties.

Up to now, there were many reports about the cold crystallization processes of PLLA [14, 25–28]. For examples, carbon nanotubes (CNTs) were compounded with PLLA via solution blending and the nonisothermal cold crystallization properties was studied [14]. It was found that the 0.1% CNTs could act as heterogeneous nucleation agents, but when CNTs loading increased up to 1%, the crystallization was inhibited. Multi-walled carbon nanotubes (MWNTs) showed a more obvious accelerating action than single-walled carbon nanotubes (SWNTs) or double-walled

✉ Changyu Han
cyhan@ciac.ac.cn

✉ Yancun Yu
yuyc@ciac.ac.cn

[1] College of Material Science and Engineering, Jilin Jianzhu University, Changchun 130118, China

[2] Key Laboratory of Polymer Ecomaterials, Changchun Institute of Applied Chemistry, Chinese Academy of Sciences, Changchun 130022, China

carbon nanotubes (DWNTs). Zhao et al. [25] prepared PLLA/nucleating surface montmorillonite (NMMT) blends and studied the cold crystallization behavior. Both the isothermal and nonisothermal cold crystallization processes of PLLA were accelerated by increasing the NMMT contents, indicative of the nucleating effect of the NMMT. Naffakh et al. [26] investigated nonisothermal cold crystallization behavior of PLLA/tungsten disulfide inorganic nanotubes (INT-WS_2) nanocomposites in detail by varying INT-WS_2 loading. It was found that the addition of INT-WS_2 significantly increased the crystallization rate and reduced the total cold crystallinity of PLLA, indicative of remarkable nucleation-promoting effect of INT-WS_2 on the cold crystallization of PLLA. Wu et al. [27] drew a conclusion about cold crystallization of PLLA/clay nanocomposites. At the low heating rate, the cold crystallization of PLLA nanocomposites preceded by regime III kinetics. The nucleation effect of clay promoted the crystallization to some extent, while the impeding effect of clay resulted in the decrease in crystallization rate. At the high heating rate of 10 °C min^{-1}, crystallization preceded mainly by regime II kinetics. The formation of much more incomplete crystals in the nanocomposites with high clay loadings led to the higher degree of crystallinity and lower melting point in contrast to that of neat PLLA. Moreover, previous research work also showed that the isothermal cold crystallization rates of PLLA were faster in the PLLA/poly(D-lactide) (PDLA) blends than in neat PLLA, indicating the nucleating agent effect of the stereocomplex formed in the blends [28].

In previous work [19], a novel eggshell powder with nucleating surface (NES) to increase melt crystallization rate of PLLA was obtained through a chemical reaction between calcium carbonate on the surface of eggshell powder and phenylphosphonic acid (PPOA). Then, NES was introduced into PLLA matrix by simple melt blending to form PLLA/NES composites. Differential scanning calorimetry (DSC) and FTIR spectroscopy identified the reaction between eggshell powder and PPOA and formed PPCa on the surface of eggshell. The isothermal melt crystallization rate of the PLLA dramatically enhanced after incorporation of NES. At the same time, melt processing window of these composites become wider. The mechanical properties of nucleated PLLA were also improved attributing to the reinforcement of NES. Interestingly, the NES increased the enzymatic hydrolysis rate of PLLA obviously.

However, these composites still remained almost amorphous after traditional injection molding or extrusion processing. Therefore, by enhancing a certain extent of crystallinity to further improve the physical and mechanical properties, the cold crystallization process of PLLA/NES composites is very necessary. The basic understanding and study of a cold crystallization behaviors and dynamics play a major role in tailoring properties of these composites. Therefore, in this study isothermal and nonisothermal cold crystallization behavior and kinetics of PLLA/NES composites were investigated using DSC and analyzed by Avrami, Ozawa, and combined Ozawa–Avrami models. Finally, the nucleation activity neat PLLA and its composites was further estimated. It is expected that these observations are of great help for development of PLLA nucleated by NES and for future application in industry.

Experimental

Materials and samples preparation

PLLA (grade 4032D, comprising about 98% L-lactide) used in this study was a commercial product from Nature Works LLC (USA). Its mass average molecular mass (M_w) and polydispersity were 2.07 × 10^5 g mol^{-1} and 1.73, respectively. The eggshell was provided by a local restaurant. PPOA was purchased from Jiaxing Alpharm Fine Chemical Co. Ltd., China.

The NES was prepared in accordance with previous work [19]. The eggshell powder and PPOA were well mixed at ambient temperature. After that, the mixture was at 180 °C of an oven to fully react for 3 min. In the current study, the NES was prepared by fixing ES/PPOA mass ratio at 5/1.

NES and PLLA were dried at 110 °C in an oven for 4 h before melt blending. PLLA/NES composites were prepared by using HaakeRheomix 600. The melt compounding was set to be at 180 °C with a screw speed of 60 rpm. Then, all the samples were further hot-pressed at 190 °C for 3 min into films with thickness of 0.4 mm and subsequently quenching into liquid nitrogen. The blend filled with various content of NES was denoted as PLLAX, where X represented the content of NES (mass%) in the composites.

Characterizations

The cold crystallization behavior was carried out by the TA Instrument differential scanning calorimeter (DSC) Q20 equipped with a Universal Analysis 2000. Sample mass varied between 5.0 and 8.0 mg. To investigate the isothermal cold crystallization behavior, the samples were heated at a heating rate of 100 °C min^{-1} to the chosen crystallization temperature and kept for some time until the isothermal crystallization was finished. The cold crystallization temperatures used in this study were from 85 to 95 °C. In nonisothermal cold crystallization, the samples were heated from 40 to 190 °C at selected heating rates ranging of 2.5, 5, 10, and 20 °C min^{-1}. All operations were carried out under nitrogen atmosphere.

Results and discussion

Isothermal cold crystallization behavior and kinetics

The effects of NES on the isothermal cold crystallization behavior of PLLA in the composites from the amorphous state were quantitatively analyzed through isothermal DSC experiments in a temperature range from 85 to 95 °C. The isothermal cold crystallization curves at different temperatures for neat PLLA and typical PLLA5 are shown in Fig. 1a, b, respectively. Clearly, the isothermal crystallization time of neat PLLA was much longer than that of the PLLA composite at a fixed crystallization temperature, confirming that the NES accelerated the isothermal cold crystallization of PLLA effectively. Figure 2a, b shows the plots of relative degree of crystallinity (X_t) against crystallization time (t) for neat PLLA and PLLA5, respectively. In the isothermal crystallization experiment, X_t at crystallization time t is defined as the ratio of the area under the exothermic curve between the onset crystallization time and t to the whole area under the exothermic curve. Figure 2a, b shows that all the curves have the similar shape of 'S'. Furthermore, the corresponding crystallization time for the neat PLLA and composites decreased with an increase in the crystallization temperature (T_c).

The crystallization time for the PLLA/NES composites becomes shorter with an increase in the NES content at a given T_c. For example, it took neat PLLA around 15.5 min to complete crystallization at 85 °C, but for the PLLA5, PLLA10, and PLLA20 samples, the time required to

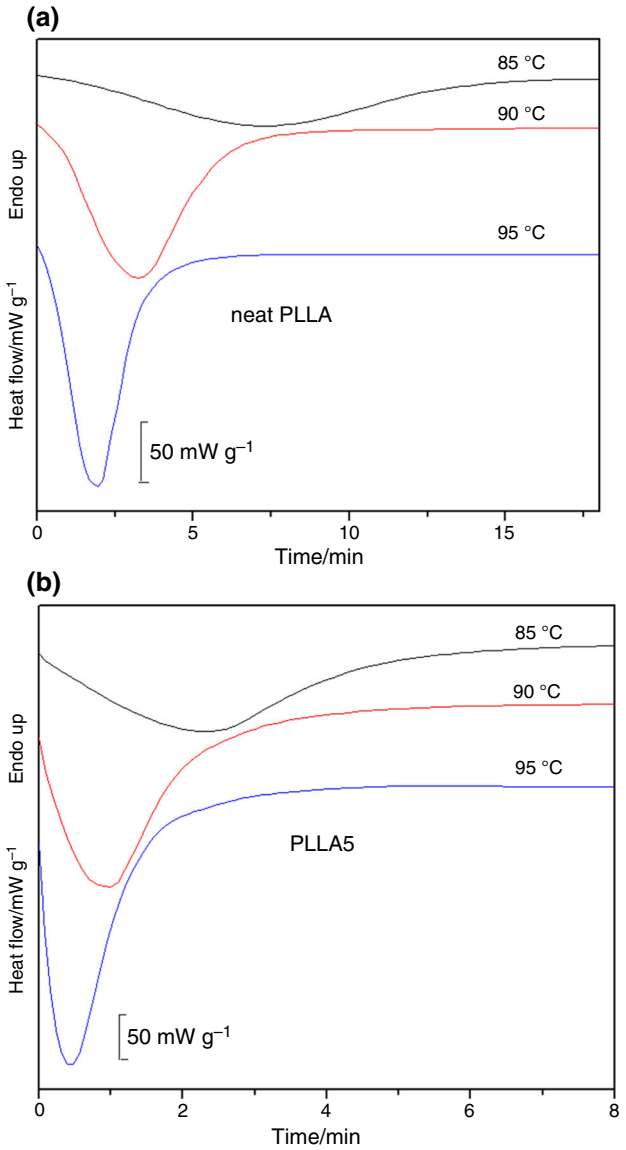

Fig. 1 DSC curves of isothermal cold crystallization at selected crystallization temperature: **a** neat PLLA, **b** PLLA5

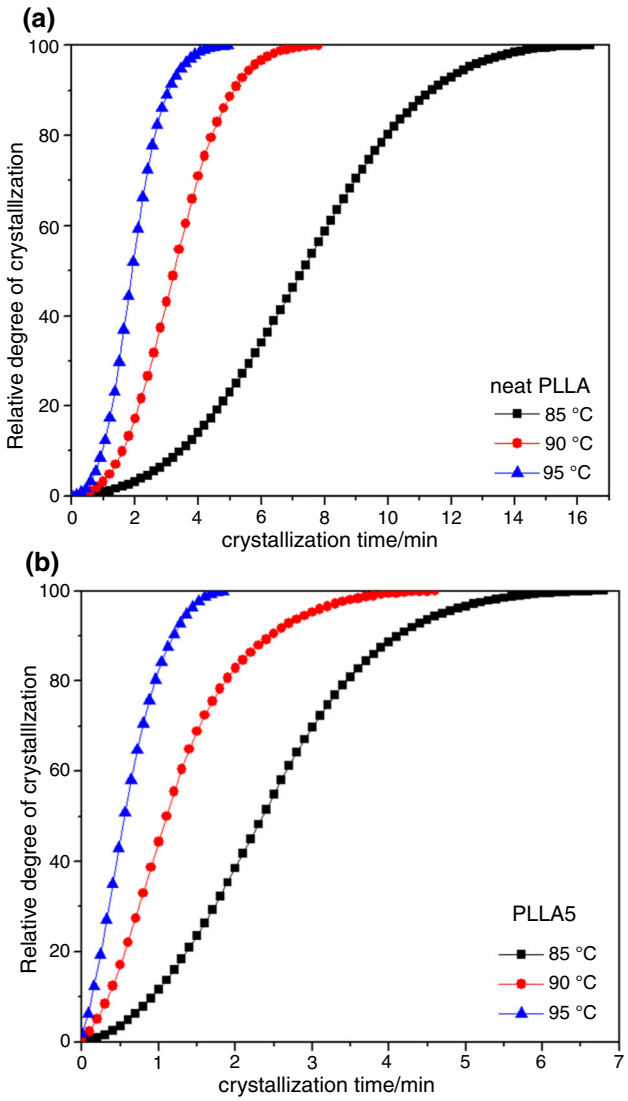

Fig. 2 The relative degree of crystallinity versus crystallization time at different crystallization temperature: **a** neat PLLA, **b** PLLA5

complete crystallization is about 6.0, 5.2, and 3.2 min, respectively. The corresponding crystallization time was summarized and is listed in Table 1.

The Avrami equation is usually adopted to analyze the isothermal crystallization kinetics of polymers, which assumed that the relative degree of crystallization X_t dependent crystallization time t may be expressed as [29, 30]:

$$1 - X_t = \exp(-Z_t t^n) \quad (1)$$

where X_t is the relative degree of crystallinity at time t, Z_t is the whole rate constant related to both nucleation and growth speed, and n is the Avrami index depending on the type of nucleation and growth geometry of the crystals [31]. Equation (2) is the linear form of Eq. (1)

$$\log(-\ln(1 - X_t)) = \log Z_t + n \log t \quad (2)$$

Figure 3a, b shows the Avrami plots of $\log(-\ln(1 - X_t))$ versus $\log t$ for neat PLLA and PLLA5, and the slopes of plots are the Avrami parameters n. The values of n for neat PLLA and PLLA/NES composites at T_c of 85, 90, and 95 °C were also summarized and are listed in Table 1. The value of n is often in the range of number from 1 to 4, which is dependent on the crystallization mechanism. It was found that the values of n were between 1.2 and 2.6, depending on the NES content and isothermal crystallization temperature. The crystallization mechanism of melt crystallization and cold crystallization was different because of different crystallization processes. In the previous work [22], the isothermal melt crystallization kinetics of neat PLLA and the PLLA/NES composites had been investigated. The value of n ranged between 2.3 and 2.9, suggesting a crystal growth of three-dimensional and spherulite morphology of heterogeneous nucleation [32].

Table 1 Isothermal cold crystallization kinetics parameters for neat PLLA and PLLA/NES composites

Sample	T_c/ °C	n	Z_t/min^{-n}	r^2	$t_{1/2}$/ min	$1/t_{1/2}$/ min^{-1}
Neat PLLA	85	2.4	5.91×10^{-3}	0.9957	7.2	0.14
	90	2.6	3.35×10^{-2}	0.9988	3.3	0.30
	95	2.6	0.12	0.9987	1.9	0.53
PLLA5	85	2.1	0.12	0.9995	2.3	0.43
	90	1.6	0.58	0.9985	1.1	0.91
	95	1.5	1.84	0.9931	0.5	2.00
PLLA10	85	1.6	0.31	0.9990	1.6	0.63
	90	1.4	1.18	0.9981	0.7	1.43
	95	1.2	2.27	0.9982	0.3	3.33
PLLA20	85	1.5	0.85	0.9988	0.9	1.11
	90	1.3	2.31	0.9939	0.4	2.50
	95	1.2	3.83	0.9968	0.2	5.00

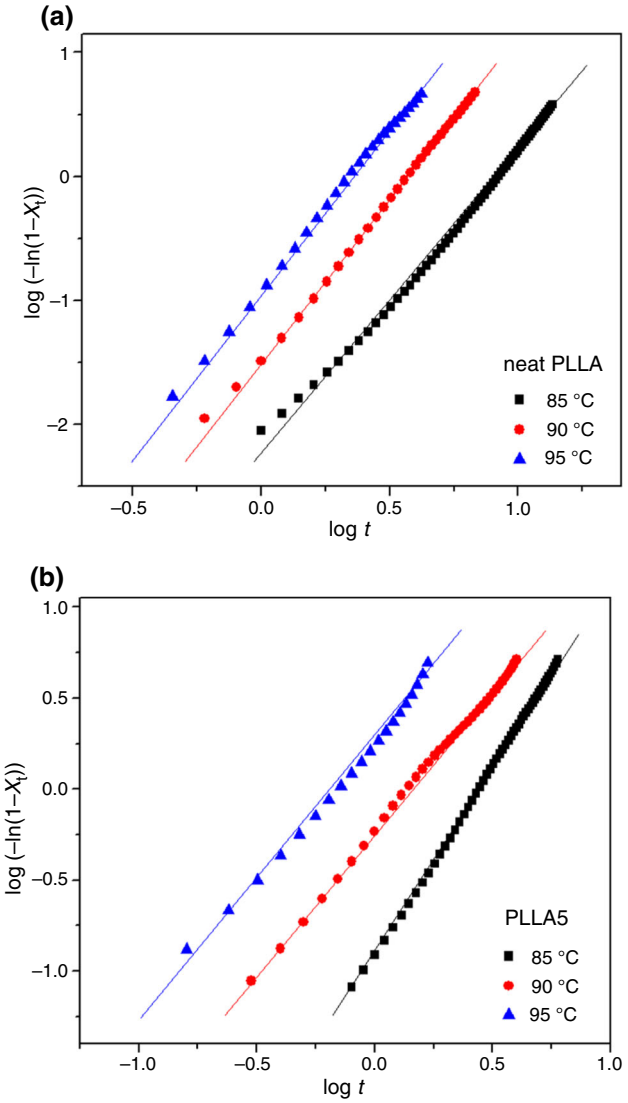

Fig. 3 Avrami plots of $\log(-\ln(1 - X_t))$ versus $\log t$ for isothermal cold crystallization: **a** neat PLLA, **b** PLLA5

Obviously, the average values of n for isothermal cold crystallization were smaller than that of melt crystallization, suggesting that the crystallization of the formulations corresponds to one or two dimensions. Therefore, the lower n values of isothermal cold crystallization could be owing to a faster crystallization rate that did not have enough time to crystallize in three dimensions [33].

The Avrami parameters Z_t for cold crystallization could be calculated directly through the intercept of the plots shown in Fig. 3, and the results are also summarized in Table 1. It was found that the Z_t values of isothermal cold crystallization increased as increasing T_c from 85 to 95 °C, indicating that crystallization process was controlled by diffusion. It was noted that because of the change in n, the Z_t (the unit was min^{-n}) values could not represent the crystallization rate completely. Therefore, the crystallization

half-time $t_{1/2}$, which is defined as the time when X_t reaches 50% and can be obtained from the plot of X_t versus t, was introduced for describing the whole crystallization rates. The $t_{1/2}$ values are listed in Table 1. Moreover, the reciprocal of $t_{1/2}$ ($1/t_{1/2}$) with T_c was also calculated and is listed in Table 1, from which the effects of the NES content and T_c on the change in crystallization rate can be obtained obviously. As we can see, the $1/t_{1/2}$ values were longer in the composites than in neat PLLA, and values $1/t_{1/2}$ increased with increasing the NES content at a given T_c, indicating that the NES acting as an nucleating agent enhanced the isothermal cold crystallization process of PLLA obviously. Moreover, the $1/t_{1/2}$ values increased with an increase in T_c for both PLLA/NES composites and neat PLLA, suggesting that the overall isothermal cold crystallization becomes faster with increasing T_c. This was attributed to the fact that a higher T_c makes the movement for chain much easier, thus resulting in the increase in the overall crystallization rate.

Nonisothermal cold crystallization behavior and kinetics

Nonisothermal cold crystallization and overall crystallization kinetics of neat PLLA and the PLLA/NES composites were carried out to further study the influence of NES on the cold crystallization behavior of PLLA in the composites. As described in the experimental section, to make sure the amorphous state of PLLA, all the samples were quenched from the melt to liquid nitrogen before measurement. The nonisothermal cold crystallization of neat PLLA and the PLLA/NES composites was studied at different heating rates to 190 °C. The major influencing factors on the nonisothermal cold crystallization of PLLA/NES composites were the NES loading and the heating rate. Figure 4a, b shows the nonisothermal crystallization curves of neat PLLA and PLLA5 at various heating rates of 2.5, 5, 10, and 20 °C min^{-1}. From these plots, the cold crystallization peak temperature (T_p) could be obtained, and the T_p values at different heating rates are summarized in Table 2. It was observed, first, that T_p increased with increasing heating rate for all the samples investigated. For example, T_p of neat PLLA increased 23.7 °C when the heating rate increased from 2.5 to 20 °C min^{-1}. Second, the presence of NES in PLLA led to T_p shifting toward higher temperatures. For example, at the heating rate of 10 °C min^{-1}, the value of T_p for neat PLLA was 108.3 °C, whereas it was 98.0, 95.1, and 91.5 °C for PLLA5, PLLA10, and PLLA20, respectively. This implied that NES was much effective in enhancing the nonisothermal cold crystallization of PLLA. Third, T_p decreased with increasing NES content, suggesting that the NES content had much effect on the degree of enhancement in T_p. As can be seen from the results

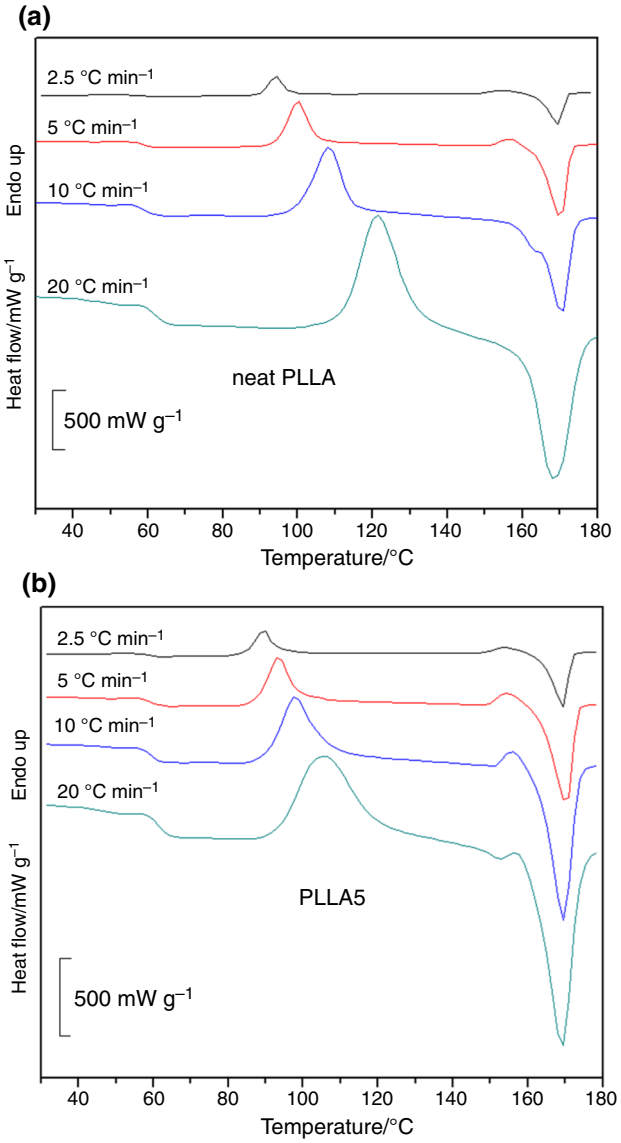

Fig. 4 DSC curves of nonisothermal cold crystallization at selected heating rates: **a** neat PLLA, **b** PLLA5

aforementioned, the nonisothermal cold crystallization of PLLA/NES composites was affected by both heating rate and the content of NES. The plots of relative degree of crystallinity as a function of crystallization temperature for neat PLLA and PLLA5 at various heating rates are illustrated in Fig. 5a, b. As expected, the higher the heating rate, the higher temperature ranged where plots shifted to. At each heating rate, the crystallization temperature of PLLA5 was lower than that of neat PLLA, which demonstrated that the presence of NES enhanced nonisothermal cold crystallization of PLLA.

In the study of nonisothermal crystallization process, the crystallization temperature can be transformed into crystallization time scale by using Eq. (3):

Table 2 Summary of nonisothermal cold crystallization parameters of neat PLLA and its blends at various heating rates

Sample	φ/ °C min^{-1}	T_p/°C	n	r^2	Z_t	$t_{1/2}$/ min	$1/t_{1/2}$/ min^{-1}
PLLA	2.5	94.6	3.9	0.9751	2.25×10^{-3}	3.9	0.26
	5	100.3	4.0	0.9875	1.70×10^{-2}	2.4	0.43
	10	108.3	4.0	0.9965	0.15	1.5	0.67
	20	118.3	4.5	0.9925	0.43	1.1	0.91
PLLA5	2.5	89.6	3.2	0.9949	1.14×10^{-2}	3.2	0.31
	5	93.6	3.2	0.9959	6.43×10^{-2}	2.0	0.50
	10	98.0	3.0	0.9963	0.42	1.2	0.85
	20	105.2	2.7	0.9954	1.52	0.8	1.28
PLLA10	2.5	87.8	2.7	0.9961	3.21×10^{-2}	3.0	0.33
	5	91.2	2.6	0.9968	0.13	1.8	0.56
	10	95.1	3.0	0.9975	0.37	1.2	0.86
	20	101.0	2.9	0.9984	1.45	0.7	1.35
PLLA20	2.5	85.5	3.3	0.9811	1.44×10^{-2}	2.9	0.34
	5	88.1	2.8	0.9975	0.14	1.7	0.58
	10	91.5	3.3	0.9969	0.64	1.0	0.97
	20	96.5	3.2	0.9977	4.03	0.6	1.72

$$t = \frac{T - T_0}{\varphi} \tag{3}$$

where T and T_0 are the temperature at crystallization time t and the initial temperature of crystallization, respectively. The φ is the heating rate. The values of $t_{1/2}$ and their reciprocal $1/t_{1/2}$ for neat PLLA and its composites are summarized in Table 2. The variations of $1/t_{1/2}$ could clearly show the influence of the NES content on the change in the crystallization rate. It could be seen that the values of $1/t_{1/2}$ increased with an increase in the NES content, indicating that the NES could enhance the nonisothermal cold crystallization rate of PLLA, as could be seen in Table 1.

It is interesting and significant for the application to study the effect of NES on the crystallization rate of PLLA in the composites quantitatively. A crystallization rate coefficient (CRC), corresponding to the change in cooling rate needed to cause 1 °C change in the supercooling of polymer melt, is frequently used to compare various polymer crystallization rate [34]. According to this model, the crystallization rates of polymer can be unified to a single scale. Plotting cooling rate against $T_m - T_p$, a straight line should be obtained, and the value of CRC can be derived from the slope. Where T_m is the melting point temperature, and T_p is nonisothermal melt crystallization peak temperature. A method modified by Qiu et al. [18], which have $T_p - T_g$ in place of $T_m - T_p$, is used to calculate CRC, because all the crystallization processes in the current work were researched from the amorphous state of PLLA. Here T_p is nonisothermal cold crystallization peak temperature, and T_g is glass transition temperature.

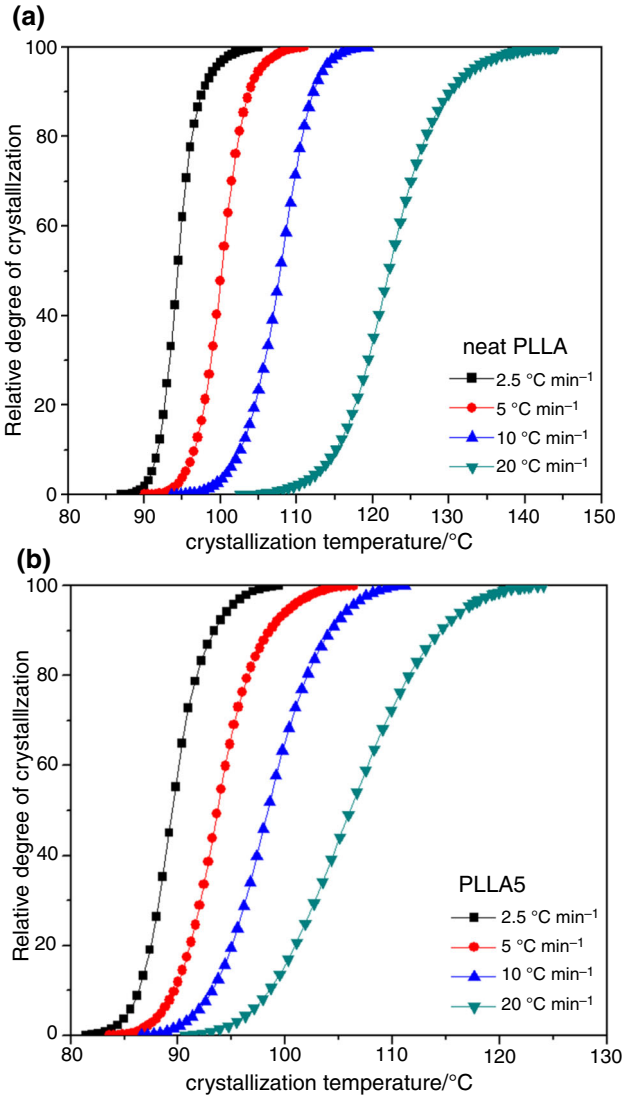

Fig. 5 The relative degree of crystallinity versus crystallization temperature at different heating rates: **a** neat PLLA, **b** PLLA5

Therefore, the method can represent a change in heating rate needed to cause 1 °C change in the superheating of amorphous phase [18]. Figure 6a gives the plots for all samples of heating rate versus $T_p - T_g$. It can be seen that, for neat PLLA, the values of CRC were around 0.836, for PLLA5 1.466, for PLLA10 1.848, and for PLLA20 2.052. The increasing values of CRC indicated that the NES enhances the nonisothermal cold crystallization process of PLLA apparently.

Zhang et al. [35–37] proposed a new concept, crystallization rate parameter (CRP), corresponding to the speed of crystallization for polymers. When $1/t_{1/2}$ is plotted against heating rate, the CRP values of neat PLLA and its composites can be determined from the slope of the line, and the higher the slope, the faster the crystallization rate will be. Figure 6b illustrates the plots of $1/t_{1/2}$ against

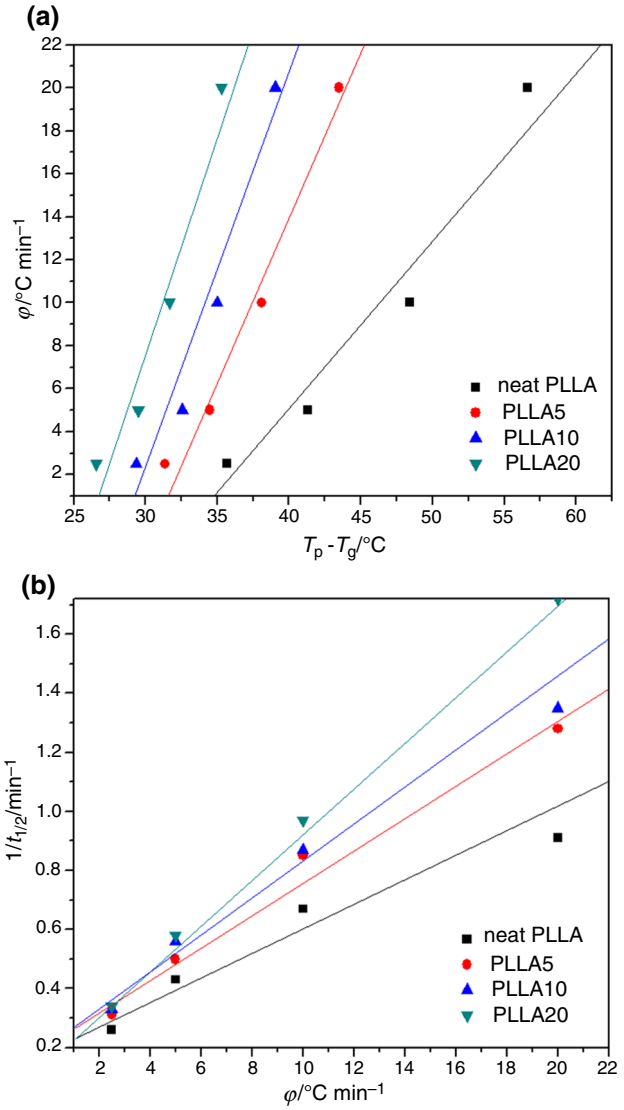

Fig. 6 Effect of the NES on the crystallization rate of PLLA: **a** crystallization rate coefficient, **b** crystallization rate parameter

heating rate for all the specimens. The values of CRP were 0.036, 0.054, 0.057, and 0.078 for neat PLLA, PLLA5, PLLA10, and PLLA20, respectively. The values of CRP were higher in the composites than in neat PLLA, indicating again that NES enhanced the cold crystallization rate of PLLA. For all the samples studied, CRP was found to increase with increasing the NES content, suggesting that cold crystallization rate of PLLA was accelerated with increasing the NES content.

Several models could be used to research the nonisothermal crystallization of polymers and composites. Jeziorny [38] modified the Avrami equation from isothermal crystallization to nonisothermal crystallization process by means of introducing the cooling rate. Figure 7a, b gives the plots of $\log(-\ln(1 - X_T))$ against $\log t$ for PLLA and PLLA5 at different heating rates. It was clear that all the plots had two distinct regions, relating to primary and secondary crystallizations. The intercept and slope of the plots for the primary crystallization regions were the Avrami parameters n and Z_t, respectively. The values of n and Z_t are listed in Table 2. Obviously, the values of n for neat PLLA was slightly larger than that of PLLA/NES composites, suggesting that the introduction of NES content may not change the mechanism of nucleation of PLLA. Additionally, the values of slope for the secondary crystallization were smaller than those of primary crystallization. The reason may be due to the transforming of spherulites growth mode from higher- to lower-dimensional space extension at the second stage, which was attributed to the spherulitic impingement and the reorganization of crystals [39].

The well-known Ozawa theory issued widely to analyze the nonisothermal crystallization kinetics [40]; it assumes that crystallization occurs at a constant cooling rate. According to Ozawa theory, the relative degree of crystallinity X_T at temperature T can be expressed as follows:

$$1 - X_T = \exp\left[\frac{-K(T)}{\varphi^m}\right] \tag{4}$$

where $K(T)$, φ, and m are the heating (or cooling) crystallization function, heating rate, and Ozawa exponent, respectively, in which Ozawa exponent m is determined by the dimension of crystal growth. The double logarithmic form of Eq. (4) can be expressed as follows:

$$\log(-\ln(1 - X_T)) = \log K(T) - m \log \varphi \tag{5}$$

Then plotting $\log(-\ln(1 - X_T))$ versus $\log \varphi$ at a given temperature, a straight line will be obtained if the Ozawa equation is valid in describing the nonisothermal crystallization kinetics. The kinetic parameters $K(T)$ and Ozawa exponent m can be calculated from the intercept and the slope of the lines, respectively. Plots based on Eq. (5) of neat PLLA and PLLA5 composites at given temperatures are illustrated in Fig. 7c, d. As shown in Fig. 7c, d, the Ozawa plots of neat PLLA and PLLA5 showed deviation from linearity, indicating that the Ozawa method was not appropriate to describe the nonisothermal crystallization of neat PLLA and PLLA/NES composites. The reason for this was probably due to the ignored assumptions of slow secondary crystallization and dependence of the fold length of polymer chain on temperature in the Ozawa equation [41].

Another approach that is adopted to analyze the nonisothermal crystallization kinetics is developed by Mo et al. [42]. The relationship between heating rate φ and crystallization time t can be set up under a certain degree of crystallinity $X(t)$ because $X(t)$ is related to φ and t, or temperature T. Therefore, by combining Avrami and

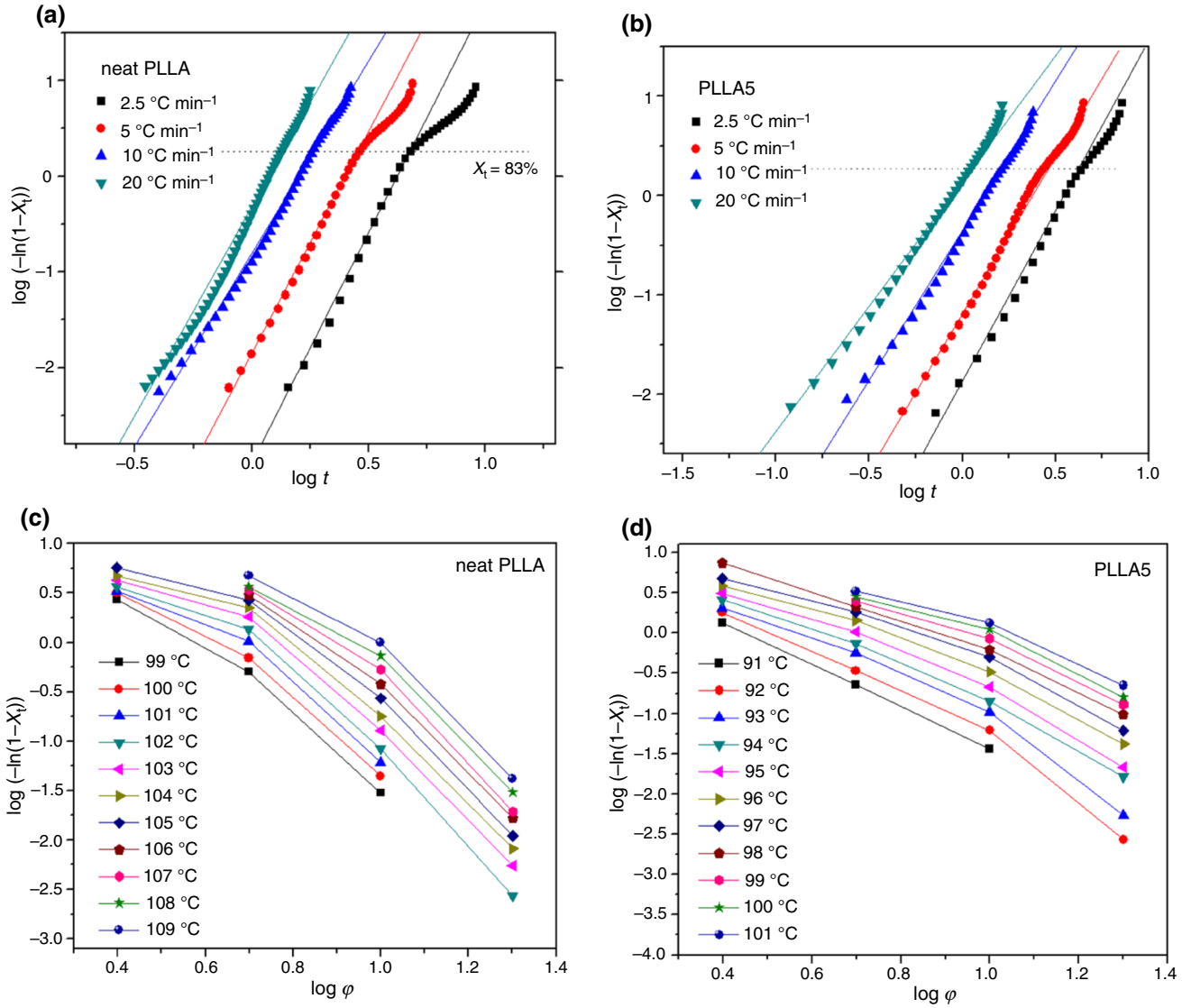

Fig. 7 Avrami plots of **a** neat PLLA, **b** PLLA5, and the Ozawa plots of **c** neat PLLA, **d** PLLA5 for nonisothermal cold crystallization

Ozawa model, a new kinetic equation for nonisothermal crystallization is created and expressed as follows:

$$\log Z_t + n \log t = \log K(T) - m \log \varphi \tag{6}$$

$$\log \varphi = \log F(T) - \alpha \log t \tag{7}$$

where $F(T) = [K(T)/Z_t]^{1/m}$ refers to the cooling rate value for a unit crystallization time when the measured system has a certain degree of crystallization. α is the ratio of the Avrami exponent to the Ozawa exponent ($\alpha = n/m$). Then, on the basis of Eq. (7), at a given degree of crystallinity, a graphic representation of log φ as a function of log t would generate a straight line, from which kinetic parameter $F(T)$ and α could be calculated from the intercept and the slope of the lines, respectively (Fig. 8). As shown in Fig. 8a, b, the combined Ozawa–Avrami model well described the nonisothermal cold crystallization to this case since the curves in the plots showed good linear relationship. The results of the kinetic parameters α and $F(T)$ are summarized in Table 3. It was found that the $F(T)$ values of PLLA/NES composites were generally smaller than those for neat PLLA, and the $F(T)$ values systematically decreased with an decrease in the relative crystallinity. Here, $F(T)$ mainly indicated the effect of NES content on the crystallization facilitation of PLLA. The value of $F(T)$ for composites was smaller than those of neat PLLA, indicating that the PLLA/NES composites had faster crystallization rate than neat PLLA at same degree of crystallinity. It was found that the values of α were almost constant for all samples, varying between 1.56 and 1.62 for neat PLLA, between 1.34 and 1.48 for PLLA5, between 1.48 and 1.55 for PLLA10, and between 1.26 and 1.31 for PLLA20. Of course, this combined Ozawa–Avrami method

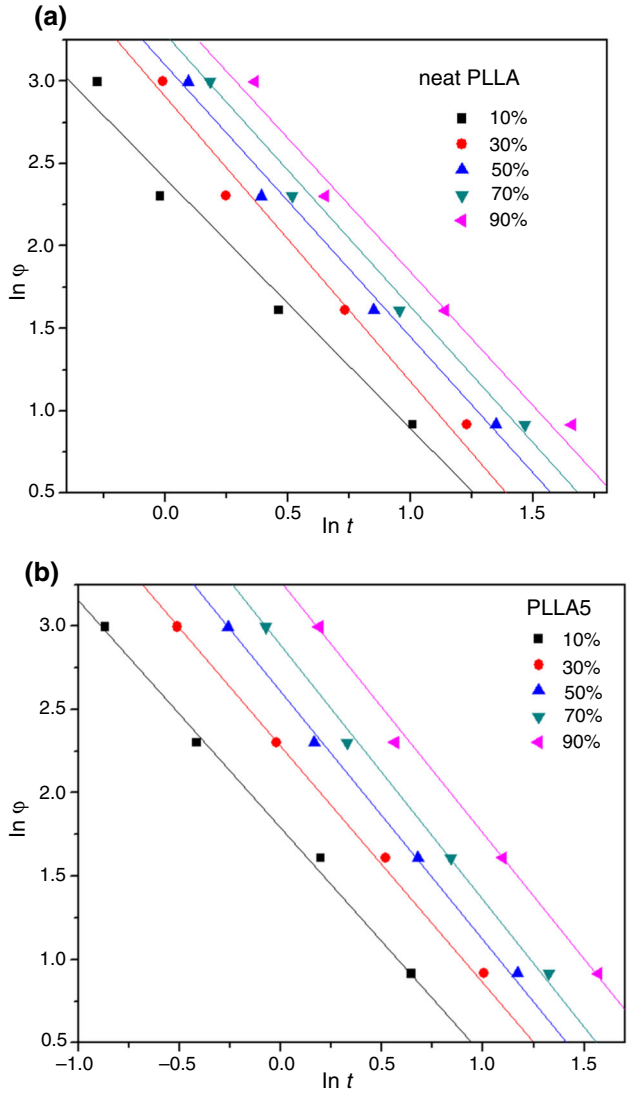

Fig. 8 Plots of ln φ against ln t for nonisothermal cold crystallization at given relative crystallinity: **a** neat PLLA, **b** PLLA5

was adequate in describing the nonisothermal crystallization of neat PLLA and its mixtures with NES, which was also valid for other polymer composites, such as poly(L-lactide)/NMMT [25], poly(lactic acid)/poly(ethylene glycol)/talc [43], PET/clay [44], and polycaprolactone/starch [45].

Nucleation activity

In order to further investigate the nonisothermal crystallization kinetics of neat and blended PLLA, a method proposed by Dobreva et al. was applied in this work to analyze the nucleating activity of a foreign substrate from polymer melt [46, 47]. When homogeneous nucleation from a melt, φ is T_p dependent as follows:

Table 3 The values of α and $F(T)$ at different relative degrees of crystallinity by combined of Ozawa–Avrami equation

Sample	X_t/%	α	$F(T)$	r^2
PLLA	10	1.56	11.22	0.9689
	30	1.62	17.23	0.9720
	50	1.62	21.08	0.9819
	70	1.60	24.78	0.9877
	90	1.56	31.51	0.9775
PLLA5	10	1.34	6.12	0.9939
	30	1.36	9.93	0.9994
	50	1.44	13.31	0.9979
	70	1.47	17.26	0.9964
	90	1.48	25.09	0.9935
PLLA10	10	1.55	5.19	0.9937
	30	1.49	9.12	0.9977
	50	1.53	12.96	0.9998
	70	1.51	17.10	0.9995
	90	1.48	25.01	0.9933
PLLA20	10	1.27	5.07	0.9942
	30	1.27	7.85	0.9967
	50	1.30	10.15	0.9965
	70	1.31	12.51	0.9980
	90	1.26	16.22	0.9973

$$\log \varphi = A - \frac{B}{2.3\Delta T_p^2} \tag{8}$$

Then, for heterogeneous nucleation

$$\log \varphi = A - \frac{B^*}{2.3\Delta T_p^2} \tag{9}$$

where A is a constant, φ is the cooling rate, and ΔT_p is the degree of superheating for cold crystallization ($\Delta T_p = T_p - T_g$). B is a parameter related to entropy of melting, specific surface energy and three-dimensional nucleation for the filled system. B^* is the value of B for the unfilled one. The values of B and B^* can be derived from the slope of the linear plots of log φ against $1/\Delta T_p^2$. Therefore, the nucleation activity (ψ) which affects the three-dimensional nucleation process can be calculated from the ratio of B^* and B ($\psi = B^*/B$). If the foreign substrate is inert for the nucleation, ψ approaches 1; on the contrary, for an active foreign substrate, ψ approaches 0. Figure 9 gives plots of log φ versus $1/\Delta T_p^2$ for neat PLLA and PLLA/NES composites. The ψ values of PLLA5, PLLA10 and PLLA20 were calculated to be 0.98, 0.96, and 0.80, respectively. According to the values of the ψ, it was found that the NES loading did not have obvious effect on the nucleation activity of PLLA/NES composites.

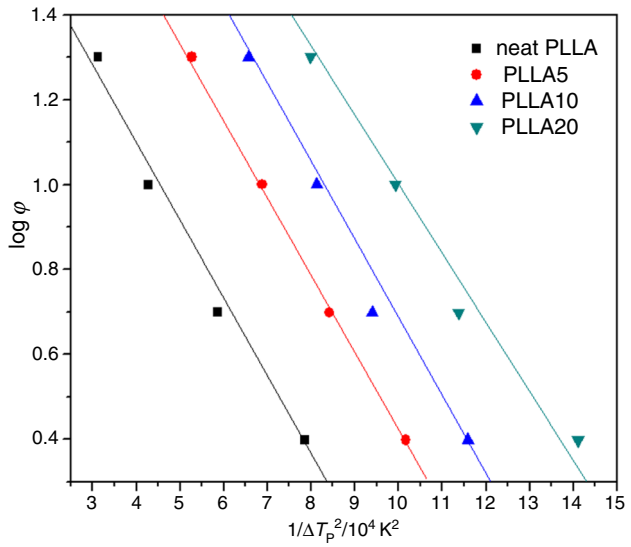

Fig. 9 The Dobreva plots of log φ versus $1/\Delta T_p^2$ for neat PLLA and its composites

Conclusions

The isothermal and nonisothermal cold crystallization behavior and kinetics of neat PLLA and melt blended PLLA/NES composites containing 2.5–20 mass% NES were studied by DSC. Isothermal cold crystallization kinetics of neat PLLA and the PLLA/NES composites were investigated at different crystallization temperatures. The overall crystallization rate was faster in the composites than in neat PLLA, which increased with increasing the NES loading. For isothermal cold crystallization studies, the crystallization of PLLA was enhanced by the presence of NES, and the enhancement was influenced by the NES loading in the composites. Nonisothermal cold crystallization kinetics of neat PLLA and its composites were also studied at different heating rates. It was found that the half-time decreased with increase in the NES loading, and crystallization exotherm moved to higher temperature range with an increase in heating rate, suggesting that both the NES loading and heating rate were the two major factors influencing the nonisothermal cold crystallization process of PLLA. In addition, Ozawa equation was rather inapplicable. In contrast, the Avrami method and combined Ozawa–Avrami model plots showed good linearity and were able to describe crystallization process for these systems. On the basis of Avrami analysis, it can be concluded that the NES may not alter the nonisothermal cold crystallization mechanism of PLLA.

Acknowledgements This work is supported by program of Cooperation of Hubei Province and Chinese Academy of Sciences, Jilin Province Science and Technology Agency (20160204030GX), program of Changchun Municipal Scientific and Technologic Development (16SS16), and Innovation team project of Beijing Institute of Science and Technology (IG201703N). Part of this work is supported by Start up Foundation for Doctors of Jilin Jianzhu University (861107) and Training Program of Innovation and Entrepreneurship for Undergraduates of Jilin Jianzhu University (2017S1011).

References

1. Garlotta D. A literature review of poly(lactic acid). J Polym Environ. 2001;9:63–84.
2. Bogaert JC, Coszach P. Poly(lactic acids): a potential solution to plastic waste dilemma. Macromol Symp. 2000;153:287–303.
3. Shi N, Dou Q. Non-isothermal cold crystallization kinetics of poly(lactic acid)/poly(butylene adipate-co-terephthalate)/treated calcium carbonate composites. J Therm Anal Calorim. 2015;119:635–42.
4. Li CL, Dou Q, Bai ZF, Lu QL. Non-isothermal crystallization behaviors and spherulitic morphology of poly(lactic acid) nucleated by a novel nucleating agent. J Therm Anal Calorim. 2015;122:407–17.
5. Kawasaki N, Nakayama A, Maeda Y, Hayashi K, Yamamoto N, Aiba S. Synthesis of a new biodegradable copolyesteramide: poly(L-lactic acid-co-ε-caprolactam). Macromol Chem Phys. 1998;199:2445–51.
6. Calandrelli L, Calarco A, Laurienzo P, Malinconico M, Petillo O, Peluso G. Compatibilized polymer blends based on PDLLA and PCL for application in bioartificial liver. Biomacromol. 2008;9:1527–34.
7. Lee JH, Park TG, Park HS, Lee DS, Lee YK, Yoon SC, Nam JD. Thermal and mechanical characteristics of poly(L-lactic acid) nanocomposite scaffold. Biomaterials. 2003;24:2773–88.
8. Chen GX, Kim HS, Shim AJ, Yoon JS. Role of epoxy groups on clay surface in the improvement of morphology of poly(L-lactide)/clay composites. Macromolecules. 2005;38:3738–44.
9. Fernández MJ, Fernández DM, Aranburu I. Poly(L-lactic acid)/organically modified vermiculite nanocomposites prepared by melt compounding: effect of clay modification on microstructure and thermal properties. Eur Polym J. 2013;49:1257–67.
10. Zhang DH, Kandadai MA, Cech J, Roth S, Curran SA. Poly(L-lactide) (PLLA)/multiwalledcarbon nanotube (MWCNT) composite: characterization and biocompatibility evaluation. J Phys Chem B. 2006;110:12910–5.
11. Quan H, Zhang SJ, Qiao JL, Zhang YL. The electrical properties and crystallization of stereocomplex poly(lactic acid) filled with carbon nanotubes. Polymer. 2012;53:4547–52.
12. Amirian M, Chakoli AN, Sui JH, Cai W. Enhanced mechanical and photoluminescence effect of poly(L-lactide) reinforced with functionalized multiwalled carbon nanotubes. Polym Bull. 2012;68:1747–63.
13. Zhao YY, Qiu ZB, Yan S, Yang WT. Crystallization behavior of biodegradable poly(L-lactide)/multiwalled carbon nanotubes nanocom-posites from the amorphous state. Polym Eng Sci. 2011;51:1564–73.
14. Chen L, Zhang JM. Nonisothermal cold crystallization of PLLA/CNTs composites. Polym Mater Sci Eng. 2012;28:64–7.
15. Fernández MD, Fernández MJ, Cobos M. Effect of polyhedral oligomeric silsesquioxane (POSS) derivative on the morphology, thermal, mechanical and surface properties of poly(lactic acid)-based nanocomposites. J Mater Sci. 2016;51:3628–42.
16. Gardella L, Basso A, Prato M, Monticelli O. PLA/POSS nanofibers: a novel system for the immobilization of metal nanoparticles. ACS Appl Mater Interfaces. 2013;5:7688–92.
17. Yu J, Qiu ZB. Preparation and properties of biodegradable poly(L-lactide) /octamethyl-polyhedral oligomeric silsesquioxanes nanocomposites with enhanced crystallization rate via simple melt compounding. ACS Appl Mater Interfaces. 2011;3:890–7.

18. Yu J, Qiu ZB. Isothermal and nonisothermal cold crystallization behaviors of biodegradablepoly(L-lactide)/octavinyl-polyhedral oligomeric silsesquioxanes nanocomposites. Ind Eng Chem Res. 2011;50:12579–86.
19. Li Y, Xin SY, Bian YJ, Xu K, Han CY, Dong LS. The physical properties of poly(L-lactide) and functionalized eggshell powder composites. Int J Biol Macromol. 2016;85:63–73.
20. Varga J, Stoll K, Menyhárd A, Horváth Z. Crystallization of isotactic polypropylene in the presence of a b-nucleating agent based on a trisamide of trimesic acid. J Appl Polym Sci. 2011;12:1469–80.
21. Menyhárd A, Varga J, Molnár G. Comparison of different b-nucleators for isotactic polypropylene, characterization by DSC and temperature-modulated DSC (TMDSC) measurements. J Therm Anal Calorim. 2006;83:625–30.
22. Molnár J, Menyhárd A. Separation of simultaneously developing polymorphic modifications by stepwise crystallization technique in non-isothermal calorimetric experiments. J Therm Anal Calorim. 2016;124:1463–9.
23. Lim LT, Auras R, Rubino M. Processing technologies for poly(lactic acid). Prog Polym Sci. 2008;33:820–52.
24. Ghosh S, Viana JC, Reis RL, Mano JF. Effect of processing conditions on morphology and mechanical properties of injection-molded poly(L-lactic acid). Polym Eng Sci. 2007;47:1141–7.
25. Zhao HW, Bian YJ, Li Y, Han CY, Dong QL, Dong LS, Gao Y. Enhancing cold crystallization of poly(L-lactide) by a montmorillonitic substrate favoring nucleation. Thermochim Acta. 2014;588:47–56.
26. Naffakh M, Marco C, Ellis G. Non-isothermal cold-crystallization behavior and kinetics of poly(L-lactic acid)/WS_2 inorganic nanotube nanocomposites. Polymers. 2015;7:2175–89.
27. Wu DF, Wu L, Wu LF, Xu B, Zhang YS, Zhang M. Nonisothermal cold crystallization behavior and kinetics of polylactide/clay nanocomposites. J Polym Sci Part B Polym Phys. 2007;45:1100–13.
28. Li Y, Han CY. Isothermal and nonisothermal cold crystallization behaviors of asymmetric poly(L-lactide)/poly(D-lactide) blends. Ind Eng Chem Res. 2012;51:15927–35.
29. Avrami M. Granulation, phase change, and microstructure kinetics of phase change. III. J Chem Phys. 1941;9:177–84.
30. Avrami M. Kinetics of phase change. II. Transformation-time relations for random distribution of nuclei. J Chem Phys. 1940;8:212–24.
31. Kamal MR, Chu E. Isothermal and nonisothermal crystallization of polyethylene. Polym Eng Sci. 1983;23:27–31.
32. Tsuji H, Tezuka Y. Stereocomplex formation between enantiomeric poly(lactic acid)s. 12. Spherulite growth of low-molecular-weight poly(lactic acid) s from the melt. Biomacromol. 2004;5:1181–6.
33. Vasanthan N, Ly H, Ghosh S. Impact of nanoclay on isothermal cold crystallization kinetics and polymorphism of poly(L-lactic acid) nanocomposites. J Phys Chem B. 2011;115:9556–63.
34. Khanna YP. A barometer of crystallization rates of polymeric materials. Polym Eng Sci. 1990;30:1615–9.
35. Zhang R, Zheng H, Lou X, Ma D. Crystallization characteristics of polypropylene and low ethylene content polypropylene copolymer with and without nucleating agents. J Appl Polym Sci. 1994;51:51–6.
36. Park JY, Kwon MH, Lee YS, Park OO. Effects of nucleating agent on nonisothermal crystallization of syndiotactic polystyrene. Korean J Chem Eng. 2000;17:262–5.
37. Wu M, Yang GZ, Wang M, Wang WZ, Zhang WD, Feng JC, Liu TX. Nonisothermal crystallization kinetics of ZnO nanorod filled polyamide 11 composites. Mater Chem Phys. 2008;109:547–55.
38. Jeziorny A. Parameters characterizing the kinetics of the nonisothermal crystallization of poly(ethylene terephthalate) determined by DSC. Polymer. 1978;19:1142–4.
39. Chen EC, Wu TM. Isothermal and nonisothermal crystallization kinetics of nylon 6/functionalized multi-walled carbon nanotube composites. Polym Eng Sci. 2010;46:1309–17.
40. Ozawa T. Kinetics of non-isothermal crystallization. Polymer. 1971;12:150–8.
41. Cho J, Baratiana S, Kim J, Yeh F, Hsiao BS, Runt J. Crystallization and structure formation of poly(L-lactide-co-meso-lactide) random copolymers: a time-resolved wide- and small-angle X-ray scattering study. Polymer. 2003;44:711–7.
42. Liu TX, Mo ZS, Wang SE, Zhang HF. Nonisothermal melt and cold crystallization kinetics of poly(aryl ether ether ketone ketone). Polym Eng Sci. 1997;37:568–75.
43. Li M, Hu DF, Wang YM, Shen CY. Nonisothermal crystallization kinetics of poly(lactic acid) formulations comprising talc with poly(ethylene glycol). Polym Eng Sci. 2010;50:2298–305.
44. Wang YM, Shen CY, Li HM, Li Q, Chen JB. Nonisothermal melt crystallization kinetics of poly(ethylene terephthalate)/clay nanocomposites. J Appl Polym Sci. 2004;91:308–14.
45. Wang Y, Rodriguez-Perez MA, Reis LR, Mano JF. Thermal and thermomechanical behaviour of polycaprolactone and starch/polycaprolactone blends for biomedical applications. Macromol Mater Eng. 2005;290:792–801.
46. Dobreva A, Gutzow I. Activity of substrates in the catalyzed nucleation of glass forming melts. I. Theory. J Non-Cryst Solids. 1993;162:1–12.
47. Dobreva A, Gutzow IJ. Activity of substrates in the catalyzed nucleation of glass forming melts. II. Experimental evidence. J Non-Cryst Solids. 1993;162:13–25.